GEOPHYSICAL RESEARCH LETTERS, VOL. 27, NO. 9, PAGES 1239-1242, MAY 1, 2000

Satellite Microwave SST Observations of Transequatorial Tropical Instability Waves

Dudley B. Chelton[1], Frank J. Wentz[2], Chelle L. Gentemann[2], Roland A. de Szoeke[1] and Michael G. Schlax[1]

Abstract. Satellite measurements of sea-surface temperature (SST) by the TRMM Microwave Imager reveal previously unreported features of tropical instability waves (TIWs). In the Pacific, TIW-related variability is observed from the eastern boundary to at least 160°E. Cusp-shaped distortions of SST fronts and associated trains of anticyclonic vortices both north and south of the equator propagate westward at ~0.5 m s^{-1} with approximately 50% larger meridional displacements in the north. In the Atlantic, TIWs and associated anticyclonic vortices are clearly observed only on the north side of the equator where they propagate from the eastern boundary to the western boundary at ~0.3 m s^{-1}.

Introduction

Early satellite observations of sea-surface temperature (SST) in the Pacific [*Legeckis*, 1977; *Legeckis et al.*, 1983] and Atlantic [*Legeckis and Reverdin*, 1987] exposed the existence of westward-propagating waves a few degrees north of the equator with wavelengths of 1000-2000 km, periods of 20-40 days and phase speeds of 0.3-0.6 m s^{-1} [*Qiao and Weisberg*, 1995]. Models and observations conclude that these waves are generated by instabilities of the equatorial currents [e.g.,*Philander*,1978; *Cox*, 1980; *Luther and Johnson*, 1990]. The waves are thus referred to as tropical instability waves (TIWs).

A diagnostic feature of instability analyses of equatorial currents is that the fastest-growing waves should be transequatorially coherent with larger amplitude north of the equator and approximately symmetric phase of meridional velocity perturbations [e.g., *Yu et al.* 1995]. This implies approximately antisymmetric pressure perturbations. To the extent that velocity streamlines coincide with isotherms, SST perturbations should also have equatorially antisymmetric phase structure.

The predicted southern signatures of TIWs have not previously been reported from SST. This is perhaps due to limited data coverage because the tropics are cloud covered about 60% of the time [*Hahn et al.*, 1995], thus obscuring SST from the infrared sensors that have been available for satellite measurements of SST. Here we investigate the evolution of TIWs from satellite microwave observations which are capable of measuring SST in nearly all weather conditions.

[1]College of Oceanic and Atmospheric Sciences, Oregon State University, Corvallis

[2]Remote Sensing Systems, Santa Rosa, California

Paper number 1999GL011047.
0094-8276/00/1999GL011047$05.00

The Evolution of TIWs

Since December 1997, the TRMM (Tropical Rainfall Measuring Mission) Microwave Imager (TMI) has been observing the Earth over the 10.7-85.0 GHz range of the microwave spectrum [*Kummerow et al.*, 1998]. The atmosphere is nearly transparent at the lower frequencies, thereby allowing measurements of SST under all weather conditions excluding rain. Rain-contaminated observations are easily identified [*Wentz and Spencer*, 1998]. A physically based algorithm is used to estimate SST at a spatial resolution of 46 km with an rms accuracy of 0.5°C [*Wentz*, 1998].

For present purposes, the SST measurements have been composite averaged over 3-day periods. TMI coverage exceeds 90% throughout most of the tropics while infrared coverage by the Advanced Very High Resolution Radiometer (AVHRR) is less than 60% over vast regions (Plate 1).

The TMI data clearly show the synoptic temporal evolution of TIWs. Consistent with previous satellite and in situ observations [*Legeckis et al.*, 1983; *Baturin et al.*, 1997], TIWs were absent during the 1997-98 El Niño. Cold water first appeared along the equator east of 140°W on 13 May 1998, signaling the demise of El Niño conditions. Within a week, an equatorial cold tongue extended west to the dateline and cusp-shaped wave patterns appeared almost immediately along its northern flank.

From animations of the TMI SST fields, (an animation of Pacific and Atlantic TIWs can be viewed from the TRMM Data page of http://www.remss.com/), the northern cusps appear to form as relatively small perturbations near the Galapagos at 92°W. They grow rapidly as they propagate west, displacing isotherms meridionally by several degrees of latitude west of about 110°W (Plate 2). Swirls of cold water rotate clockwise off the tips of many of the northern cusps, evidently indicative of anticyclonic vortices between the cusps as first observed by *Hansen and Paul* [1984] from drifter trajectories. One such vortex surveyed during 1990 extended to a depth of 150 m with a diameter of about 500 km [*Flament et al.*, 1996].

Similar cusp patterns form and propagate west along the southern flank of the Pacific cold tongue. The southern cusps become larger as the TIW season progresses (Plate 2). They were usually tipped backward like their northern counterparts, suggestive of anticyclonic vortices along the southern SST front as well.

By mid October 1998, TIWs were highly developed on both sides of the equator. Wavetrains of cusps and associated vortices propagated west at least as far as 160°E with visually indistinguishable phase speeds on opposite sides of the equator. The Pacific SST fronts and TIWs remained well defined until February 1999.

Cross-equatorial alignments are difficult to quantify since the cusps become progressively distorted with increasing dis-

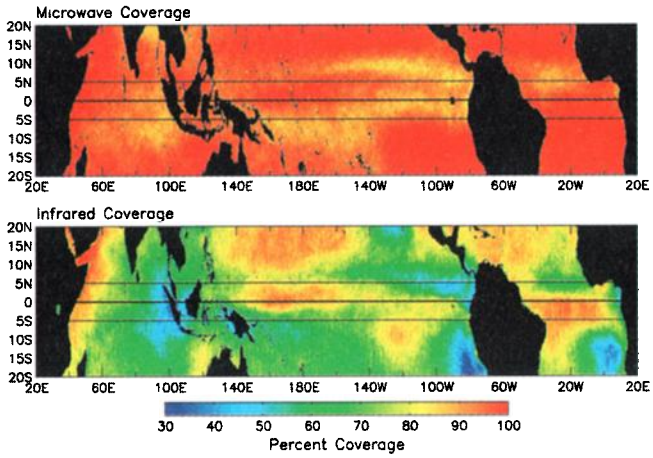

Plate 1. Percent coverage of SST measurements from the microwave TMI (upper) and the infrared AVHRR (lower) in 3-day composite-average maps during calendar year 1998.

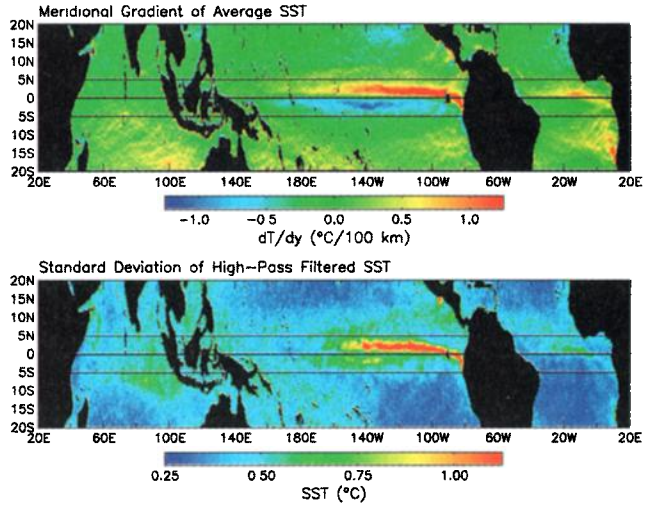

Plate 3. The meridional gradient of average SST (upper) and the standard deviation of 50-day high-pass filtered SST (lower) during the TIW season June 1998-February 1999.

tance from the equator, as previously noted for the northern cusps by *Weidman et al.* [1999]. However, the sinuous character of the cold tongue (bottom panel of Plate 2) is suggestive of antisymmetric phase structure of TIW-induced perturbations of SST.

A similar progression of SST occurred somewhat earlier in the Atlantic. Westward-propagating cusps developed along 1°N almost immediately after the appearance of equatorial cold water on 26 April 1998. As in the Pacific, the cusps appear to be associated with anticyclonic vortices. Unlike the Pacific, however, there was no clear evidence of TIWs south of the equator where SST gradients never intensified. The northern SST signatures of Atlantic TIWs became more difficult to detect after the SST front weakened in August 1998.

Cross-Equatorial Amplitude Structure

Meridional gradients of average SST ($\partial\overline{T}/\partial y$) are crucial to the detection of TIWs. In the Pacific, strong positive and negative $\partial\overline{T}/\partial y$ were associated with the SST fronts that bracket the equatorial cold tongue (Plate 3). East of 100°W, the southern front disappeared and the northern front shifted southward, crossing the equator at 90°W. In the Atlantic, there was only a northern front. In the Indian Ocean, SST gradients were too weak to detect whether TIWs existed.

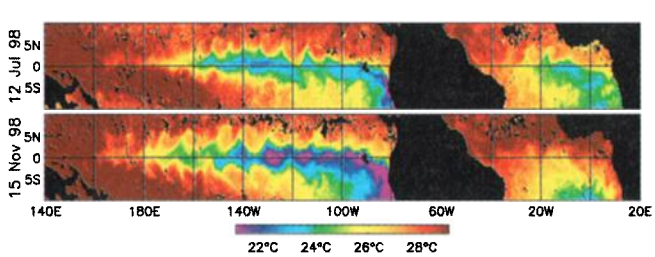

Plate 2. Selected 3-day composite-average maps of SST measured from the TMI for the periods 11-13 July 1998 (upper) and 14–16 November 1998 (lower). Black areas represent land or rain contamination.

SST variability associated with TIWs can be isolated by 50-day high-pass filtering. Areas of large-amplitude variability coincided with areas of large poleward $\partial\overline{T}/\partial y$ (Plate 3). The northern band of high SST variability in the Pacific crossed the equator following the northern SST front all the way to the eastern boundary.

West of 110°W, the amplitudes of Pacific SST variations for a given $\left|\partial\overline{T}/\partial y\right|$ were larger in the northern hemisphere (Plate 4). In the Atlantic, SST perturbations north of the equator were smaller than in the Pacific and SST variability was below the noise level south of the equator.

The slopes of straight-line fits to the scatter plots in Plate 4 are a measure of the TIW-induced meridional displacement of isotherms. Results obtained for the North Pacific, South Pacific and North Atlantic are 80, 55 and 50 km, respectively. For sinusoidally meandering isotherms, these correspond to peak-to-peak meridional displacements of 226, 156 and 141 km. Because of the cusped nature and nonstationarity of the amplitudes of TIWs, displacements can be twice as large (see Plate 2). The ratio of about 1.5 between northern and southern displacements in the Pacific is consistent with the larger northern amplitudes of TIWs predicted from instability theories.

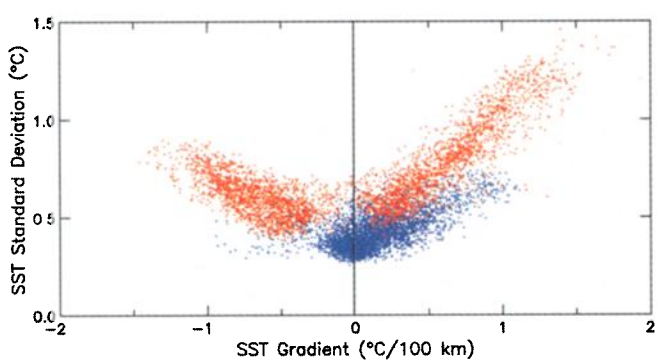

Plate 4. Scatter plot comparison between 50-day high-pass filtered SST and $\partial\overline{T}/\partial y$ for the region 110°W-160°W, 5°S-5°N in the Pacific (red dots) and the region 0-60°W, 5°S-5°N in the Atlantic (blue dots).

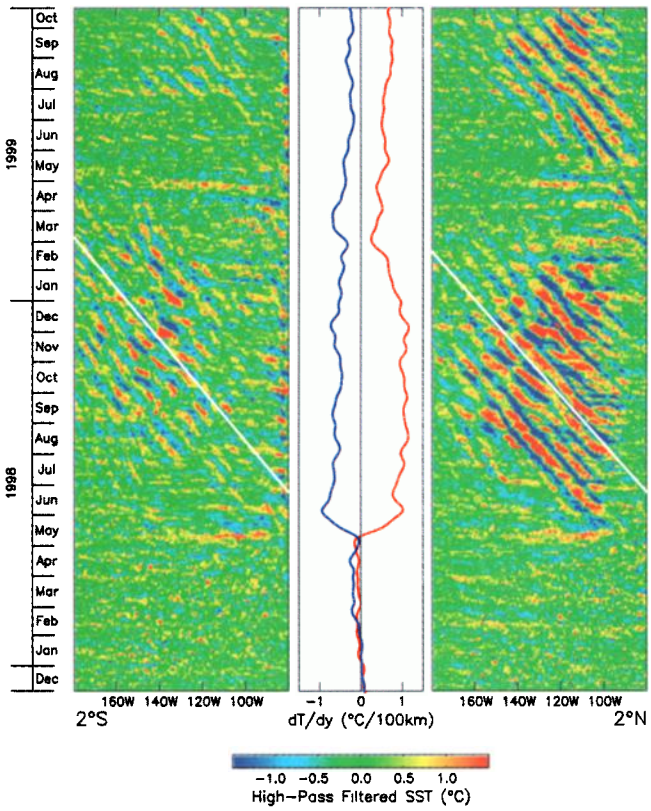

Plate 5. Time-longitude plots of 50-day high-pass filtered SST along 2°S (left) and 2°N (right). White lines represent Radon transform estimates of phase speed [*Deans*, 1993; *Chelton and Schlax*, 1996] over the time period June 1998-February 1999. Time series in the middle panel are 20-day low-pass filtered meridional SST gradients averaged over the longitude range 160°W-110°W between 3°N and the equator (red curve) and between the equator and 3°S (blue curve).

SST variability when $\partial\overline{T}/\partial y = 0$ represents measurement noise plus signals unrelated to TIWs. The zero intercepts of about 0.5°C in Plate 4 are thus an upper-bound estimate of the imprecision of 3-day composite average SST. This is consistent with the 0.5°C accuracy estimate for individual TMI measurements of SST [*Wentz*, 1998].

Discussion

The microwave measurements of SST presented here reveal previously unreported features of TIWs: SST signatures of Pacific TIWs are evident on *both* sides of the equator with about 50% larger amplitude in the north; the northern band of short-period Pacific SST variability indicates that TIW signals extend east of 100°W to the eastern boundary; Pacific TIWs propagate farther west than the dateline, perhaps all the way to the western boundary, although this cannot be determined from SST since $\partial\overline{T}/\partial y$ becomes very weak west of 160°E.

Miller et al. [1985] and *Flament et al.* [1996] have suggested that the cusp-shaped distortions of the northern SST front are caused by anticyclonic vortices between the cusps. The prevalence of cusps in the TMI data suggests that these vortices are very common on both sides of the equator in the Pacific and north of the equator in the Atlantic, apparently forming in very regular trains.

The availability of TMI data in nearly all weather conditions allows an uninterrupted record of the propagation of SST signatures of TIWs. From a time-longitude section in the Pacific (Plate 5), westward propagation along 2°N became apparent west of 100°W beginning in late May 1998, coincident with the onset of a strong $\partial\overline{T}/\partial y$. In late February 1999, westward propagation appears to have terminated west of 110°W and begun again near the eastern boundary. A phase speed of 0.53 m s^{-1} was estimated from the 50-day high-pass filtered SST (see white lines in Plate 5).

Westward propagating SST signals are also evident along 2°S (Plate 5) where small-amplitude TIWs appeared in May 1998 at the same time that TIWs appeared along 2°N. For reasons to be determined, the amplitudes of the southern SST perturbations increased considerably in late August 1998 and persisted west of 110°W for about a month longer than the northern TIWs. The phase speed estimate from the 50-day high-pass filtered SST along 2°S was 0.50 m s^{-1}, very similar to the phase speed estimate along 2°N.

Although the ~0.5 m s^{-1} signals are dominant, much faster westward propagating signals with longer wavelengths and smaller amplitudes are clearly seen superposed in both panels of Plate 5. An especially clear example occurred in late April 1999, between the two periods of energetic TIWs shown in Plate 5. The nature of these wave-like signals that have wavenumber and frequency characteristics distinctly different from those of TIWs is under investigation.

The association of SST variability with $\partial\overline{T}/\partial y$ is expected; wave-induced lateral movements of isotherms result in large SST variations at a fixed latitude when $\partial\overline{T}/\partial y$ is large. Furthermore, the strength of $\partial\overline{T}/\partial y$, as it reflects the mean zonal current structure, is itself an index of the times and locations of the potential for lateral shear instabilities that would generate TIWs. The possibility that TIWs may exist when and where $\partial\overline{T}/\partial y$ is weak could be investigated from measurements of dynamical variables such as meridional velocity or sea level.

As a case in point and consistent with previous studies, there was no evidence of propagation east of 100°W along 2°N during the 1998-99 TIW season. As noted above, the northern front and associated band of SST variability were south of 2°N in this region (Plate 3). The isolated band of SST variations along 2°S (Plate 5) over the longitude range where the northern front extends from 90°W to the eastern boundary indicates that TIW-induced SST variability existed along the entire northern front. After February 1999, TIW-induced SST variability was evident near the eastern boundary along 2°N (Plate 5) where TIWs became detectable because the northern front had shifted to the north.

Time-longitude sections in the Atlantic (not shown) are similar to the Pacific sections. SST perturbations were apparent on both sides of the equator, but with barely detectable magnitudes and intermittent presence south of the equator. The estimated phase speed along 1°N was 0.31 m s^{-1}, much slower than in the Pacific.

The South Pacific signatures of TIWs identified from TMI data are key features that provide insight into the dynamics of the waves. The suggestion of equatorially antisymmetric phase structure of SST is consistent with theoretical predictions but is inconsistent with the symmetric cross-equatorial phase structure suggested from TOPEX/POSEIDON altimetric measurements of sea surface height [*Chelton*

et al., 1999, The latitudinal structure of monthly variability in the tropical Pacific, manuscript submitted to *J. Phys. Oceanogr.*]. An effort to reconcile this apparent contradiction is the subject of ongoing research.

Acknowledgments. We thank M. Freilich and J. Lyman for comments on the manuscript. The Pathfinder AVHRR data in Plate 1 were provided by PODAAC at the Jet Propulsion Laboratory (JPL). This work was supported by NASA/JPL contract 1206715, NASA TRMM contract NAS5-9919 and NASA's Earth Science Information Partnership through contract SUB1998-101 from the University of Alabama at Huntsville.

References

Baturin, N. G., and P. P. Niiler, Effects of instability waves in the mixed layer of the equatorial Pacific, *J. Geophys. Res., 102,* 27,771-27,793, 1997.

Chelton, D. B., and M. G. Schlax, Global observations of oceanic Rossby waves, *Science, 272,* 234-238, 1996.

Cox, M., Generation and propagation of 30-day waves in a numerical model of the Pacific, *J. Phys. Oceanogr., 10,* 1168-1186, 1980.

Deans, S. R., *The Radon Transform and Some of its Applications*, John-Wiley, 1993.

Flament, P. J., S. C. Kennan, R. A. Knox, P. P. Niiler and R. L. Bernstein, The three-dimensional structure of an upper ocean vortex in the tropical Pacific Ocean, *Nature, 383,* 610-613, 1996.

Hahn, C. J., S. G. Warren and J. London, The effect of moonlight on observation of cloud cover at night, and application to cloud climatology, *J. Climate, 8,* 1429-1446, 1995.

Hansen, D. V., and C. A. Paul, Genesis and effects of long waves in the equatorial Pacific. *J. Geophys. Res., 89,* 10,431-10,440, 1984.

Kummerow, C., W. Barnes, T. Kozu, J. Shiue, and J. Simpson, The Tropical Rainfall Measuring Mission (TRMM) Sensor Package, *J. Atmos. Ocean Technol., 15,* 808-816, 1998.

Legeckis, R., Long waves in the eastern equatorial Pacific Ocean: A view from a geostationary satellite, *Science, 197,* 1179-1181, 1977.

Legeckis, R., and G. Reverdin, Long waves in the equatorial Atlantic Ocean during 1983, *J. Geophys. Res., 92,* 2835-2842, 1987.

Legeckis, R., W. Pichel, and G. Nesterczuk, Equatorial long waves in geostationary satellite observations and in a multichannel sea surface temperature analysis, *Bull. Am. Meteorol. Soc., 64,* 133-139, 1983.

Luther, D. S., and E. S. Johnson, Eddy energetics in the upper equatorial Pacific during Hawaii-to-Tahiti Shuttle Experiment. *J. Phys. Oceanogr., 20,* 913-944, 1990.

Miller, L., D. R. Watts, and M. Wimbush, Oscillations of dynamic topography in the eastern equatorial Pacific, *J. Phys. Oceanogr., 15,* 1759-1770, 1985.

Philander, S. G. H., Instabilities of zonal equatorial currents, Part 2, *J. Geophys. Res., 83,* 3679-3682, 1978.

Miller, L., D. R. Watts, and M. Wimbush, Oscillations of dynamic topography in the eastern equatorial Pacific, *J. Phys. Oceanogr., 15,* 1759-1770, 1985.

Qiao, L., and R. H. Weisberg, Tropical instability wave kinematics: Observations from the Tropical Instability Wave Experiment, *J. Geophys. Res., 100,* 8677-8693, 1995.

Weidman, P. D., D. L. Mickler, B. Dayyani and G. H. Born, Analysis of Legeckis eddies in the near-equatorial Pacific, *J. Geophys. Res., 104,* 7865-7887, 1999.

Wentz, F. J., Algorithm Theoretical Basis Document: AMSR Ocean Algorithm, *Tech. Rept. 110398,* Remote Sensing Systems, Santa Rosa, CA, November 1998.

Wentz, F. J., and R. W. Spencer, SSM/I rain retrievals within a unified all-weather ocean algorithm, *J. Atmos. Sci., 55,* 1613-1627, 1998

Yu, Z., J. P. McCreary, and J. A. Proehl, On the meridional asymmetry and energetics of tropical instability waves, *J. Phys. Oceanogr., 25,* 2997-3007, 1995.

D. Chelton, R. de Szoeke and M. Schlax, College of Oceanic and Atmospheric Sciences, Oregon State University, Corvallis, OR 97331-5503 (e-mail: chelton@oce.orst.edu; szoeke@oce.orst.edu)

F. Wentz and C. Gentemann, Remote Sensing Systems, 438 First Street, Suite 200, Santa Rosa, CA 95401 (e-mail: wentz@remss.com; gentemann@remss.com)

(Received September 13, 1999; revised November 12, 1999; accepted December 21, 1999.)